IOP Conf. Series: Materials Science and Engineering **249** (2017) 012017 doi:10.1088/1757-899X/249/1/012017

Microscopic bubble behaviour in suppression pool during wetwell venting

G Zablackaite, H Nagasaka, H Kikura

Laboratory for Advanced Nuclear Energy, Institute of Innovative Research, Tokyo Institute of Technology, 2-12-1-N1-7, Ookayama, Meguro-ku, Tokyo Japan

zablackaite.a.aa@m.titech.ac.jp

Abstract. During a severe accident PCV failure should be avoided and fission products inside PCV should be confined as much as possible. In order to minimize FPs release, Wetwell venting is conducted by releasing steam-non-condensable gas mixture carrying FPs from the Drywell to Suppression Pool. Steam is condensed by subcooled water in the pool, and most of FPs are retained into water. The removal of FP in the water pool is referred to as "Pool Scrubbing effect". Hydrodynamic parameters of bubbles have impact on pool scrubbing effect. However, there is only few data available to evaluate quantitatively the bubble behaviour under depressurization and/or thermal stratification conditions. Series of experiments were conducted to evaluate the influence of temperature distribution, non-condensable gas content and pressure in the Wetwell on bubble behaviour. Bubbles were visualized using High Speed Camera and adopting shadowgraphy technique. Applying Particle Tracking Velocimetry, bubble velocity and size distribution were obtained from recorded images. Experimental results show that with increasing suppression pool temperature, bubbles reaching the pool surface decreased in size and traveling velocity became slower. In pressurized wetwell, bubble behaviour was similar to that in the heated up suppression pool case, although bubble parameters were similar to the low temperature case. Higher air content induced water surface movement and bubbles were smaller due to break up.

1. Introduction

One of the ways to prevent Primary Containment Vessel (PCV) failure during severe accident is to actuate containment venting [1]. The pressure inside the containment is decreased by opening flow paths to the outside. However, venting may lead to direct release of fission products (FPs) to the environment. In order to reduce the risk, benefits of pool scrubbing effect can be used in Boiling Water Reactors (BWR).

In the case of Reactor Pressure Vessel failure, increased pressure in the Drywell (D/W) is reduced by conducting Wetwell (W/W) venting by releasing mixture of steam and non-condensable gas to the Suppression Pool (S/P) via vent pipes. Big bubbles form at the outlet of the downcomer pipe, detach and rise. Large bubble starts to collapse and breaks to many small bubbles. When the steam within the bubble reaches the surface of the bubble, condensation occurs and bubble decrease in size. On the other hand, rising bubble without condensing steam expands due to the decreasing water head towards the surface of the pool. Fission products, trapped inside the bubbles, are expected to be captured in the water once it reaches the interface of the bubble surface and water. The removal of FP in the water pool is referred to as "Pool scrubbing effect".

On March 11, 2011, the Great East Japan Earthquake caused the accident in Fukushima Daiichi Nuclear Power Plant [2]. The Station Blackout resulted in the core meltdown and the explosion of reactor building at Unit 1 and 3. A great amount of radioactive materials was released to the environment. Because of loss of AC/DC power, reactor cooling systems failed. Pressure inside containment vessel started to rise and several PCV venting were conducted in Unit 1 and in Unit 3. Mixture of steam and non-condensable gases with fission products (FPs) flew into wetwell. Non-condensable gases passed through the pool and reached the surface of water. Large amount of steam increased the temperature of the pool and it was suggested that thermal stratification occurred above the exit of vent pipe. Analysis of Radiation Monitoring data shows large peaks of radiation after initiated W/W venting, which demonstrates that pool scrubbing was not as effective as expected [3]. The efficiency of scrubbing effect under depressurization and thermal stratification was remarkably reduced. Hence, more analysis is needed to fully understand the effect of venting conditions on FPs release to environment and how efficiency of pool scrubbing effect was reduced during Fukushima Daiichi accident [4].

Hydrodynamic parameters of bubble have impact on pool scrubbing effect. However, there is only few recent available data to evaluate quantitatively the bubble behavior. Many experiments on pool scrubbing effect were conducted in 80's and 90's. Hakii *et.al.* [5] analyzed influence of parameters, such as injection nozzle diameter, scrubbing depth, and steam fraction in carrier gas, for pool scrubbing. Kulhman *et.al.* [6] tested the influence of FP size and water temperature for decontamination factor. They noticed the importance of bubble diameter and its rise velocity for FP retention. Hydrodynamic behavior of S/P was analyzed in THAI facility [7], [8]. Dependency of bubble size on downcomer pipe diameter and the injected gas flow rate was analyzed. Formation and disappearance of thermal stratification in suppression pool was experimentally analyzed by Yamauchi *et.al.* [9], and Bo *et.al* [10]. In a scaled-down torus shaped suppression pool, they observer thermal stratification above the outlet. Reduced subcooling temperature did not allow steam bubbles to condensate effectively, which led to strong mixing and dissipation of stratification. Previously conducted experiments provide good results leading to better understanding of basic pool scrubbing phenomena. However, most of the studies analyze steam or steam-air injections under constant and atmospheric pressure. Also, high flow rate causes mixing in the pool. In the case of the severe accident, especially during wetwell venting, pressure is changing, and under this condition, bubble behaviour differs. The lack of experimental data for depressurization and thermal stratification conditions does not allow to accurately evaluate the influence of hydrodynamic bubble parameters on retention of FPs in the pool under these conditions.

In this paper, experimental results of temperature distribution in S/P, air content and pressure in the W/W influence on steam-air bubble behaviour in suppression pool under different conditions are presented. The main long-term goals of the study are to observe bubble behaviour, to measure bubble size change, and traveling time to reach pool surface during BWR wetwell venting under depressurization and/or thermal stratification conditions. Therefore, the effect of bubble behaviour on pool scrubbing should be clarified.

2. Test facility

2.1. Description of the test facility

The designed test facility (Figure 1) consists of two pressure vessels – drywell (D/W) and wetwell (W/W), downcomer pipe, steam generator, air compressor, heat exchanger and High speed camera (HSC) and light source. Water temperature in the wetwell can be changed by steam injection using wetwell bypass line, and circulation pump is used to get initial uniform pool water temperature.

D/W vessel is 1.2 m long, 0.345 m in diameter. The vessel has a layer of rock wool insulation. W/W is 2.5 m high and 0.355 m in diameter (design pressure 0.6 MPa). Observation windows on the W/W vessel are arranged to observe bubble behaviour at 3 different positions above the pool floor. Downcomer submergence can be changed by changing water level and/or length of the pipe. There are

3 possible downcomer diameters and two possible downcomer lengths (Table 1). Presented cases were conducted using 12.48 mm diameter downcomer.

Table 1. Possible submergence and size of downcomer pipe.

Submergence, m	Downcomer diameter ID, mm
0.7	12.48
0.95	35.08
1.4	52.48

The piping lines are divided into main line with wetwell bypass line, S/P overflow line, W/W water inlet/outlet line and circulation line, discharge/SRV line. S/P overflow line allows to keep water level in the vessel constant. Pressure reducing valve (PRV) on the discharge line allows to keep the W/W pressure constant or depressurize the vessel. Discharge line is connected with SRV lines on D/W and W/W and the heat exchanger. Circulation line with installed magnetic pump is used to obtain uniform temperature distribution in W/W for experiments without thermal stratification.

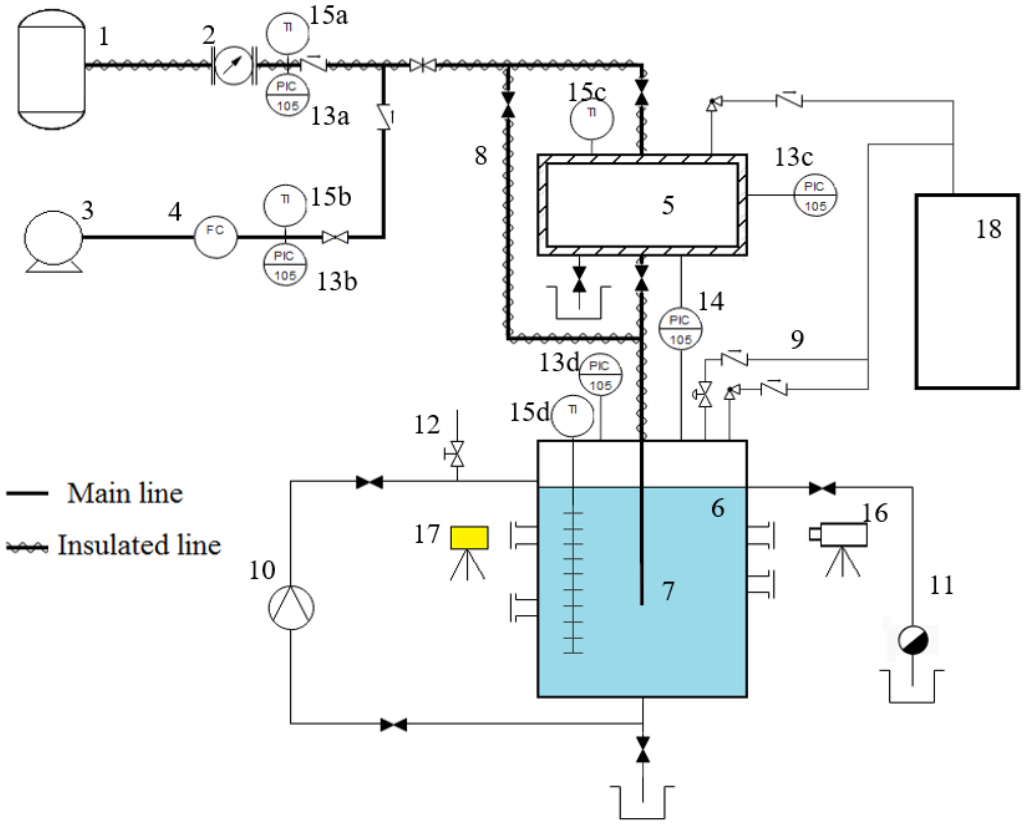

Figure 1. Schematic diagram of the test facility. 1 – steam generator; 2 – vortex flow meter; 3 – air compressor; 4 – air flow regulator; 5 – drywell; 6 – wetwell; 7 – vent line (downcomer pipe); 8 – wetwell bypass line; 9 – gas discharge line; 10 – circulation line/circulation pump; 11 – overflow line/steam trap; 12 – water supply line; 13 – pressure gauge; 14– differential pressure gauge; 15 – thermocouples; 16 – High Speed Camera; 17 – light source; 18 – heat exchanger.

2.2. Instrumentation

Pressure in D/W ($P_{D/W}$) and W/W ($P_{W/W}$) is measured by pressure transducers Panasonic DPH-L113V (measurement accuracy – 2% of the full scale). Pressure on the steam and air lines is measured by pressure transducers Panasonic DPH-L113 (measurement accuracy – 2% of the full scale). Differential

pressure gauge Yokogawa DPharp EJA110 (measurement accuracy – 0.2% of the full scale) is used to measure pressure difference between D/W and W/W. Steam flow rate ($\dot{M}_s$) is measured using TLV EF73 vortex flow meter (measurement accuracy for the low flow rate – 10% of the full scale), air flow rate is measured and regulated with PFM5 flow switch (measurement accuracy – 3 % of the full scale). Temperature in D/W ($T_{D/W}$) and on the air line is measured with a K-type thermocouple (measurement error – 2.2°C), steam line temperature (T_{st}) is measured with a T-type thermocouple (measurement error – 1°C). 10 K-type thermocouples are used to measure temperature in the W/W and to evaluate thermal stratification after steam-air release. Three thermocouples are installed below downcomer outlet (T1-T3), one thermocouple is at the outlet level (T4) and six thermocouples are above the outlet, but below water surface. Temperature is measured 7 cm away from the wall of the vessel to avoid the thermal boundary layer caused by the cooling of the non-insulated W/W. Data is recorded using Yokogawa MX100 data logger.

2.3. Bubble tracking

Bubble observation was performed adopting shadowgraphy technique. Bubbles were recorded using 2 High Speed Cameras (HSCs) and, on the opposite side of the W/W, a metal halide lamp was positioned to illuminate the inside of the vessel. The camera Photron Mini AX50 (500 fps, 1/25000 shutter speed, image resolution 1024x1024) was used to observe bubble behavior at the pool surface. The other camera Photron Fast Cam 1024 PCO, model 1KC (500fps, 1/1000 shutter speed, image resolution 1024x1024) was used to observe bubble formation at the downcomer outlet. Images were analyzed using MATLAB R2017b built-in toolboxes. The size of forming bubble at the downcomer outlet was obtained manually measuring selected images. Bubbles around the pool surface and its boundaries were automatically detected and tracked in each frame. Then, bubble velocity and size were obtained.

3. Initial conditions

Initial conditions of experimental Runs are given in Table 2. Five experiments were conducted under one parameter change. For all the cases, inner diameter of downcomer was 12.48 mm. It allowed to have more uniform size of the bubbles around the pool surface for simplified case. Submergence was set to 1.4 m, which corresponds to submergence in Fukushima Daiichi Unit 3. Bubbles were observed at two positions: around downcomer exit and around pool surface. Size of initial forming bubbles and rising bubbles at the top of pool surface were compared. W/W pressure was close to atmospheric for the Runs 1, 2, 3, and 5.

Table 2. Test matrix.

Run number	1 (ref.)	2	3	4	5
Downcomer ID, mm	12.48 (3/8")	12.48 (3/8")	12.48 (3/8")	12.48 (3/8")	12.48 (3/8")
Submergence, m	1.4[a]	1.4	1.4	1.4	1.4
Position of observation	Downcomer exit/Pool surface	Downcomer exit/Pool surface	Downcomer exit/Pool surface	Downcomer exit/Pool surface	Downcomer exit/Pool surface
W/W pressure, MPag	0.04	0.04	0.04	0.30	0.04
S/P temperature, °C	38.3	36.5-76.3	65.8	44.3	30.5
S/P temperature distribution	Uniform	Thermal stratification	Uniform	Uniform	Uniform
Steam flow rate, kg/h	2.77	2.77	2.77	18.71	5.69
Air content	4.92%	4.92%	4.92%	4.79%	22.02%

[a] - corresponding to submergence in Fukushima NPP Unit 3.

For the Run 4 W/W pressure was increased by closing discharge line and increasing the mass flow rates of steam and air. S/P temperature was changing from 30.5 °C to 76.3 °C. Runs 1, 3, 4, and 5, were done

having uniform S/P temperature, and the Run 2 was carried out in thermally stratified condition above the downcomer exit. Steam mass flow rate was set observing the differential pressure between D/W and W/W and bubble formation at the downcomer exit. Target air content was 5% in the Runs 1, 2, 3, and 4, and it was 20% in the Run 5. However, due to sensitivity of the flow regulating valves only close values were achieved.

4. Experimental procedure

After the test facility was prepared for operation, piping lines were heated up by steam release. By opening steam and air lines, D/W was heated up and remaining air from the vessel was purged. At the same time S/P was heated up releasing steam-air mixture to the W/W. Pool water was recirculated to get uniform temperature in S/P for the runs with uniform temperature distribution. For the case with thermal stratification, release of steam-air mixture was carried on without recirculating the pool. Steam and air flow rates were set to obtain predetermined air content, avoiding high pressurization of D/W. Value of differential pressure between D/W and W/W was almost equal the pressure corresponding to water head in the downcomer. After the required conditions in S/P pool were set, images of forming bubbles at the downcomer outlet and bubbles reaching the pool surface were recorded with HSCs.

5. Results and discussion

5.1. Bubble behaviour

In the case of low uniform temperature (Run 1), bubbles slid up along the downcomer pipe. Number of bubbles was small (Figure 2 (a)), and big bubbles were observed frequently. Bubbles were rising close to the downcomer. Assuming that most of the steam condensed around the outlet of downcomer due to high subcooling, bubbles contained mostly air. Big bubbles reaching the surface of the pool could have been caused by bubble coalescence after detachment from the downcomer outlet, and by decreasing water head. Bubbles collided and coalesced, and become stable enough to avoid breaking up before reaching the pool surface. The case 1 was followed by case 2 and case 3. Temperature profile in the S/P and position of termocouples are shown in Figure 3.

Thermal stratification started to develop from the beginning of steam-air mixture release to the S/P (Run 2). Due to low mass flow rate, steam-air mixture did not penetrate S/P water below downcomer outlet and mixing was not induced. Two distinct temperature layers can be seen in the temperature profile (Figure 3 (a)). Temperature T4 at the downcomer outlet level showed the boundary between two layers. Bubbles travelled only through higher temperature region. Therefore, bubbles were affected by thermal stratification layer around the outlet of downcomer, where the temperature gradient was high. Going further from the outlet, temperature was increasing evenly. Bubbles were forming in a ring shape, and started to break up around the outlet. The size of bubbles tented to change further due to break up and coalescence. Bubbles dispersed away from the downcomer (Figure 2 (b)).

In the case of higher uniform temperature (Run 3), rising bubbles dispersed further to the periphery of the vessel (as much as it was possible to see through the window). With increasing pool temperature, steam condensation rate decreased and number of bubbles increased (Figure 2 (c)). Most of the bubbles were small in size. Bigger bubbles were appearing only occasionally, which implies that even after the collision and coalescence, bubbles were not stable enough to stay big and broke up. Due to decreased rising bubble velocity, bubbles were staying at the pool surface.

In the pressurized W/W (Run 4), pool temperature was kept low, therefore, as in the first case, steam mostly condensed around the outlet of the downcomer. Only few big bubbles were observed and they were smaller in size comparing with the case 1 (Figure 2 (d)). Although, bubbles were not fast enough to break the water surface. After small bubbles reached the pool surface, majority of them were stopped or even bounced back from the interface of water. Bubble behaviour around the water surface in pressurised W/W was similar to the case with higher temperature in the S/P.

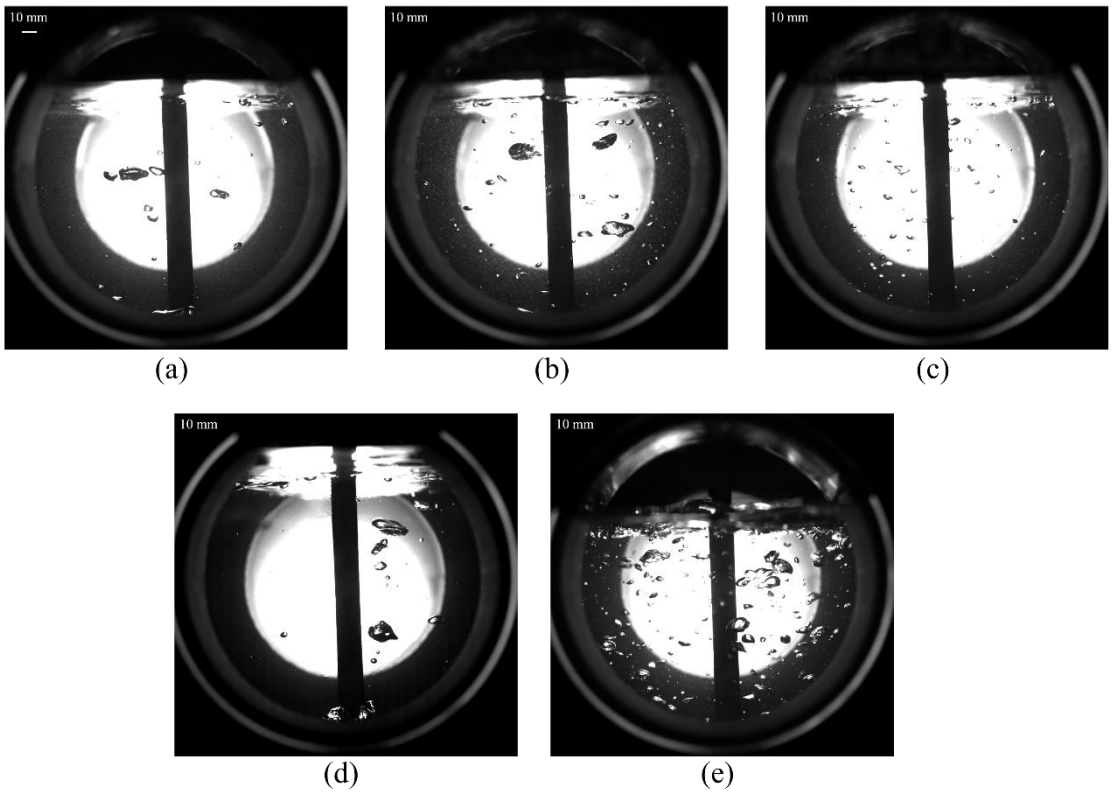

Figure 2. Bubble images close to the pool surface: (a) – low S/P temperature; (b) – stratified S/P; (c) – high S/P temperature; (d) – pressurized W/W; (e) – higher air ratio.

Having high air content (Run 5), the number of bubbles reaching the surface distinctly increased (Figure 2 (e)). Bubbles were forming faster and detaching from the downcomer outlet more frequently. Higher mass flow rate of the steam-air mixture induced movement of the pool surface. Rising bubbles strongly dispersed in the radial direction around the pool surface. Bubbles were colliding and breaking up a lot, although coalescence was observed even before the bubble reached the pool surface.

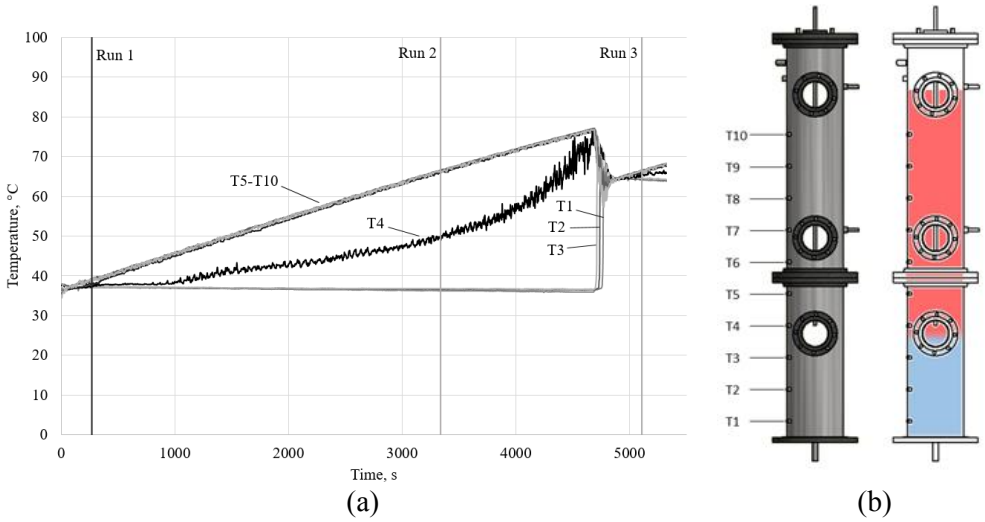

Figure 3. S/P in cases 1, 2 and 3: (a) – temperature profile, (b) – position of thermocouples in the W/W with temperature distribution in the case of thermal stratification.

5.2. Bubble size and velocity

Velocity and size distribution for all cases is given in Figure 4. Average size of forming and rising bubbles, and velocity of the rising bubbles around the pool surface are given in Table 3. The smallest detectable size of the bubbles was assumed to be 2 mm. In the low temperature S/P (Run 1), the size of formed bubble at the downcomer outlet was 18.3 mm. Average size of rising bubbles was 6.7 mm. Rising bubble size around the pool surface ranged up to 33.4 mm, although majority of the bubbles were smaller than 10 mm (Figure 4 (a)). Bubble velocity mostly ranged from 0.20 m/s to 0.55 m/s. Average velocity of rising bubbles was 0.353 m/s.

In the stratified S/P (Run 2), the size of forming bubble increased to 21.7 mm. Bubble size in this case was 4.8 mm on average, with the maximum size of 23.3 mm. Majority of the bubbles were smaller than 8 mm (Figure 4 (b)). Bubbles tended to travel slower, 0.317 m/s on average. Bubble velocity changed in the same range as in the Run 1.

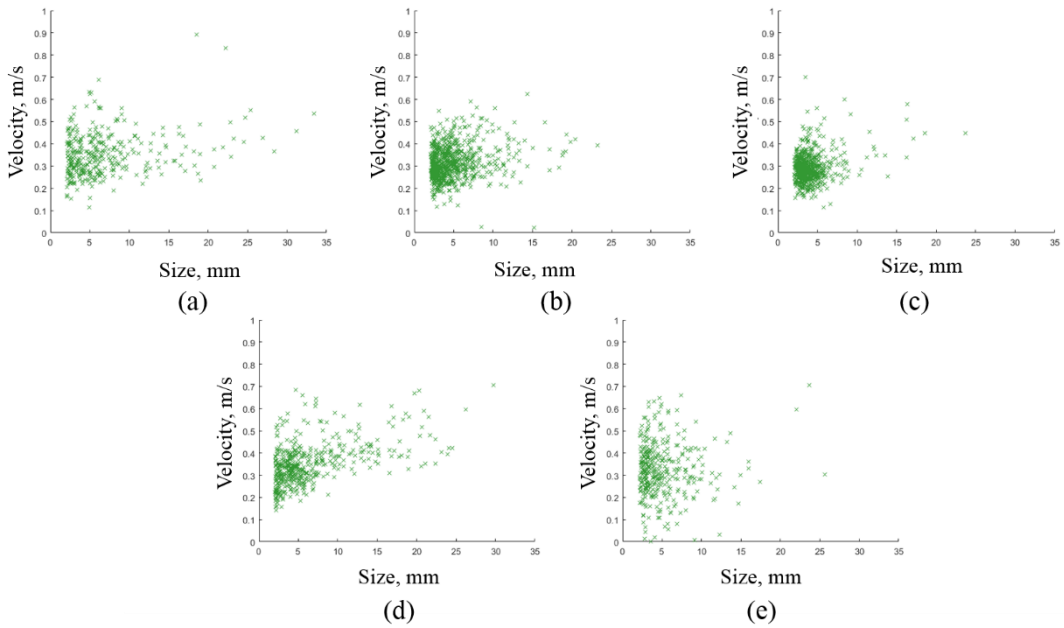

Figure 4. Size and velocity distribution around the pool surface: (a) – low S/P temperature; (b) – stratified S/P; (c) – high S/P temperature; (d) – pressurized W/W; (e) – higher air ratio.

In the high temperature S/P (Run 3), the size of formed bubble was 24.6 mm. Bubble size around the pool surface was 4.0 mm on average, with the maximum size of 23.7 mm. Bubbles around the pool surface were more uniform in size, majority of the bubbles were smaller than 6 mm (Figure 4 (c)). Comparing low and high temperature cases, the velocity of bubbles decreased, and on average it was 0.291 m/s. The velocity mostly ranged from 0.2 m/s to 0.4 m/s.

Table 3. Size and velocity.

Run number	1 (ref.)	2	3	4	5
Initial bubble size at the downcomer exit, mm	18.3	21.7	24.6	21.3	19.9
Average bubble size around pool surface, mm	6.7	4.8	4.0	6.4	5.1
Max size around pool surface, mm	33.4	23.3	23.7	29.8	25.6
Average bubble velocity around pool surface, m/s	0.353	0.317	0.291	0.352	0.320

In the pressurized W/W (Run 4), formed bubbles were 21.3 mm in size. Bubbles reaching the pool surface were 6.4 mm size on average, maximum detected size was 29.8 mm. Majority of the bubbles were smaller than 7 mm (Figure 4 (d)). Size and velocity distribution in this case is similar to the Run 1 (Figure 4 (a)), solely bigger bubbles were traveling slightly faster. Otherwise, velocity of bubbles was similar as in the first case, 0.352 m/s on average.

Lastly, in the higher air content case (Run 5), forming bubbles were 19.9 mm in size (Figure 4 (e)). In this case, bubble size reaching the surface was 5.1 mm on average, and maximum size was 25.6 mm. Bubbles were mostly smaller than 10 mm. Rising bubble velocity varied in a bigger range than in other cases. It changed from 0.1 m/s up to 0.7 m/s. Bubbles travelled at 0.320 m/s velocity on average.

6. Conclusion

Rising bubble behaviour was observed in Suppression Pool under different initial conditions. Experimental data was analyzed to evaluate the effect of S/P thermal stratification, air content in steam-air mixture, and pressure on bubble behaviour. With increasing S/P temperature, forming bubble size increased while bubbles were colliding and breaking up more easily. Therefore, the size and velocity of the bubbles decreased. Bubbles dispersed away from the downcomer pipe to the radial direction in the pool. The smallest and the slowest bubbles were observed in the case of the highest temperature S/P. In the pressurised W/W bubble parameters were similar to the low S/P temperature case. Although bubble behaviour around the water surface was resembling to the high temperature S/P. Bubbles stayed and floated at the pool surface before collapsing. High air content induced unstable movement of the pool surface by rising bubbles, although bubble size was smaller due to increased probability of break up.

References

[1] Dana L Kelly 1991 Overview of containment venting as an accident mitigation strategy in US light water reactors *Nuclear Engineering and Design* **131** 253-61
[2] AESJ, The Fukushima Daiichi Nuclear Accident Final Report of the AESJ Investigation Committee, Springer, (2014).
[3] TEPCO. The 4th Progress Report on the Investigation and Examination of Unconfirmed and Unresolved Issues on the Development Mechanism of the Fukushima Daiichi Nuclear Accident. TEPCO Progress report, (2015).
[4] Mizokami Sh, Yamada D, Honda T, Yamauchi D and Yamanaka Y 2016 Unsolved issues related to thermal-hydraulics in the suppression chamber during Fukushima Daiichi accident progression *Journal of Nuclear Science and Techology* **53** 630-8
[5] Hakii J, Kaneko I, Fukusawa M, Yamashita M and Matsumoto 1990 Experimental study on aerosol removal efficiency for pool scrubbing under high Temperature Steam Atmosphere *Proceeding of the 21st DOE/NRC nuclear air cleaning conference* **2** 21-0918
[6] Kulhman M R, Gieseke J A, Merilo M and Oehlberg R 1985 *Proceeding of American Nuclear Society meeting on fission-product behaviour and source term research* Scrubbing of fission product aerosol in LWR water pool under severe accident conditions. Experimental Results 633-48
[7] Gupta S, Schmidt E, Laufenberg B, Freitag M, Poss G, Funke F and Weber G 2015 THAI test facility for experimental research on hydrogen and fission product behavior in light water reactor containments *Nuclear Engineering and Desing* **294** 183-201
[8] Gupta S 2015 Experimental Investigation relevant for hydrogen and fission product issues raised by the Fukushima accident *Nuclear Engineering and Technology* **47** 11-25
[9] Yamauchi D, Jo B, Erkan N, Takahashi Sh, Sagawa W and Okamoto K 2016 Verification of thermal stratification characteristics using scaled-down suppression pool of the Fukushima Daiichi nuclear power plants *Mechanical Engineering Letters* **2** 16-00092
[10] Jo B, Erkan N, Takahashi Sh, Song D, Sagawa W and Okamoto K 2016 Thermal stratification in a scaled-down suppression pool of the Fukushima Daiichi nuclear power plant *Nuclear Engineering and Design* **305** 39-50